



PAPER

## Bearing fault diagnosis based on variational mode decomposition and total variation denoising

To cite this article: Suofeng Zhang *et al* 2016 *Meas. Sci. Technol.* **27** 075101

View the [article online](#) for updates and enhancements.

### You may also like

- [4D Monte Carlo dose calculations for pre-treatment quality assurance of VMAT SBRT: a phantom-based feasibility study](#)  
Natalia F Roberts, Matthew Williams, Lois Holloway et al.
- [Daily edge deformation prediction using an unsupervised convolutional neural network model for low dose prior contour based total variation CBCT reconstruction \(PCTV-CNN\)](#)  
Yingxuan Chen, Fang-Fang Yin, Zhuoran Jiang et al.
- [Sparsity-constrained PET image reconstruction with learned dictionaries](#)  
Jing Tang, Bao Yang, Yanhua Wang et al.

**ECS**  
The  
Electrochemical  
Society  
Advancing solid state &  
electrochemical science & technology

**DISCOVER**  
how sustainability  
intersects with  
electrochemistry & solid  
state science research

# Bearing fault diagnosis based on variational mode decomposition and total variation denoising

Suofeng Zhang, Yanxue Wang, Shuilong He and Zhansi Jiang

School of Mechanical and Electrical Engineering, Guilin University of Electronic Technology, Guilin 541004, People's Republic of China

E-mail: [yan.xue.wang@gmail.com](mailto:yan.xue.wang@gmail.com) (Y Wang)

Received 2 February 2016, revised 20 April 2016

Accepted for publication 22 April 2016

Published 13 May 2016



## Abstract

Feature extraction plays an essential role in bearing fault detection. However, the measured vibration signals are complex and non-stationary in nature, and meanwhile impulsive signatures of rolling bearing are usually immersed in stochastic noise. Hence, a novel hybrid fault diagnosis approach is developed for the denoising and non-stationary feature extraction in this work, which combines well with the variational mode decomposition (VMD) and majoriation–minimization based total variation denoising (TV-MM). The TV-MM approach is utilized to remove stochastic noise in the raw signal and to enhance the corresponding characteristics. Since the parameter  $\lambda$  is very important in TV-MM, the weighted kurtosis index is also proposed in this work to determine an appropriate  $\lambda$  used in TV-MM. The performance of the proposed hybrid approach is conducted through the analysis of the simulated and practical bearing vibration signals. Results demonstrate that the proposed approach has superior capability to detect roller bearing faults from vibration signals.

Keywords: variational mode decomposition, weighted kurtosis index, rolling element bearing, denoising, fault diagnosis

(Some figures may appear in colour only in the online journal)

## 1. Introduction

Rolling element bearings are widely applied in rotating machinery and play an important role in modern manufacturing industries. The failure of rolling element bearings results in the deterioration of machine performance; it is thus necessary to accurately detect faults in the bearings [1, 2]. Vibration signal analysis is the most commonly used approach due to its easy measurement and high correlation with structural dynamics [3–6]. However, there are two challenging issues in vibration signal analysis: the non-stationary collected signals and signatures usually mingled with heavy noise caused by coupled machine components and the working environment [7, 8].

For the past few years, a range of methods have been developed to analyze the measured non-stationary vibration signals in the fields of fault diagnosis. For example, wavelet transform

(WT) becomes a powerful tool for feature extraction because of its advantage of multi-resolution analysis [9, 10]. Yan [10] presented a review of the recent developments and applications of WT in the fields of fault diagnosis of rotary machines. Actually, similarity between the wavelet basis function and the defect-related signal characteristics plays a decisive role for successful detection. Thus, wavelet basis function should be appropriately selected in the WT. Nevertheless, it is sometimes not practical for a specific application. Some adaptive signal decomposition techniques emerge as the time requires, for example, empirical mode decomposition (EMD) pioneered by Huang in [11]. Subsequently, EMD technique finds wide applications in the fault diagnosis of rotating machines [12–14], due to its good intrinsic locally adaptive property in processing non-stationary signals. However, EMD still has some drawbacks, such as mode mixing and end effects. Rilling *et al* [15, 16] first completely probed into these issues of EMD.

Chen and Wang [17] presented a new analytical mode decomposition theorem based on the Hilbert transform which can address a number of issues associated with EMD. Ensemble empirical mode decomposition (EEMD), an extended version of EMD, has been developed to overcome the mode mixing of EMD in [18]. However, in order to reduce the errors caused by added white noise in EEMD, the algorithm of EMD should be conducted many times, which inevitably results in a large amount of computation burden [19]. The empirical wavelets transform (EWT) is proposed as a new adaptive data analysis method in [20], which could also partially address the limitations (sensitivity to noise and sampling) of EMD [21]. But EWT relies on robust preprocessing for peak detection, and the constructed frequency bands are still slightly strict.

Variational mode decomposition (VMD) has been lately proposed by Dragomiretskiy and Zosso [21]. Unlike the EMD, VMD is a non-recursive signal processing method with a pretty firm theoretical foundation. Meanwhile, its performances of non-stationary signal analysis have been thoroughly studied and compared with other adaptive signal processing techniques. For example, the equivalent filter bank property of the VMD has been investigated in [22], and the results show that VMD can be considered as a wavelet packet decomposition or a generalized short-time Fourier transform with a varying window width. It is also demonstrated that VMD is more powerful in tone-separation and noise robustness in comparison with EMD [23]. In addition, feature vectors extracted by VMD are better than those achieved by EWT, which is much more suitable for the support vector machine based classifications [24]. Due to the advantages of VMD, it has been successfully utilized for identifying rubbing faults [25], instantaneous detection of voiced/non-voiced regions in speech signals [23] as well as trends analysis of financial markets [26], etc. However, VMD is still not appropriate for analysis of a vibration signal with strong background noise [21]. The presence of strong noise in the measured vibration signal is unavoidable. It is thus necessary to carry out denoising preprocessing of the raw signals prior to the VMD analysis.

In practice, in order to extract a true signal in noise, the most frequently used methods are based on filters. Unlike traditional low-pass filter denoising, total variation denoising (TVD) is actually defined based on an optimization problem. TVD was initially proposed by Rudin and was applied to remove noise in images [27]. Since then, TVD has been widely researched and extensively adopted in one-dimensional (1D) signal processing [28–30] due to its advantages in preserving the sharp edges of the given signals. Since the output of the TVD is obtained by minimizing a particular cost function, TVD has been further developed with the majorization–minimization algorithm (TV-MM) [31]. It has been demonstrated that it can take little time for TV-MM to achieve a good de-noising result [32]. Nevertheless, it is also worth noting that the regularization parameter  $\lambda$  used in TV-MM could seriously affect its denoising performance.

Consequently, a hybrid approach based on TV-MM and VMD techniques for bearing fault diagnosis is proposed in this work. The weighted kurtosis index is also first proposed

to determine an appropriate  $\lambda$  used in TV-MM. The rest of this paper is organized as follows: TV-MM and VMD are briefly introduced in section 2. The weighted kurtosis index is proposed to select parameter  $\lambda$  in section 3, where its performances in denoising are also compared with the morphological filter technique through simulated bearing vibration signals. In section 4, the effectiveness of the proposed approach is further verified using the practical bearing vibration signals. Conclusions are drawn in section 5.

## 2. Background

### 2.1. A brief introduction of VMD

VMD can non-recursively decompose a multi-component input signal into a discrete set of quasi-orthogonal band-limited intrinsic mode functions (IMFs) (BLIMFs) [21], which are in accordance with the new definition of IMF described in [33]. Each mode  $u_k$  is almost compact around a matching center frequency  $\omega_k$ , and its bandwidth is assessed by means of  $H^1$  Gaussian smoothness.

The process of VMD can be considered as a constrained variational problem, while the formulation of the constrained variational problem is written [21]:

$$\min_{\{u_k\}, \{\omega_k\}} \left\{ \sum_{k=1}^K \left\| \partial_t \left[ \left( \delta(t) + \frac{j}{\pi t} \right) * u_k(t) e^{-j\omega_k t} \right] \right\|_2^2 \right\}$$

subject to  $\sum_{k=1}^K u_k(t) = f(t)$  (1)

The solution to equation (1) can be easily achieved via an unstrained optimization problem using the augmented Lagrangian method [21]

$$\mathcal{L}(\{u_k\}, \{\omega_k\}, \lambda) = \alpha \sum_{k=1}^K \left\| \partial_t \left[ \left( \delta(t) + \frac{j}{\pi t} \right) e^{-j\omega_k t} \right] \right\|_2^2 + \left\| f(t) - \sum_{k=1}^K u_k(t) \right\|_2^2 + \left\langle \lambda(t), f(t) - \sum_{k=1}^K u_k(t) \right\rangle$$
 (2)

An alternating direction method of multipliers is adopted to solve equation (2). The estimated modes  $u_k$  and the corresponding updated center frequency in the frequency domain can be written as follows:

$$\hat{u}_k^{n+1}(\omega) = \frac{\hat{f}(\omega) - \sum_{i < k} \hat{u}_i^{n+1}(\omega) - \sum_{i > k} \hat{u}_i^n(\omega) + \frac{\hat{\lambda}^n(\omega)}{2}}{1 + 2\alpha(\omega - \omega_k^n)^2}$$
 (3)

$$\omega_k^{n+1} = \frac{\int_0^\infty \omega |\hat{u}_k^{n+1}(\omega)|^2 d\omega}{\int_0^\infty |\hat{u}_k^{n+1}(\omega)|^2 d\omega}$$
 (4)

where  $\alpha$  is the balancing parameter of the data-fidelity constraint. More specifically, the process of VMD can be summarized as follows:



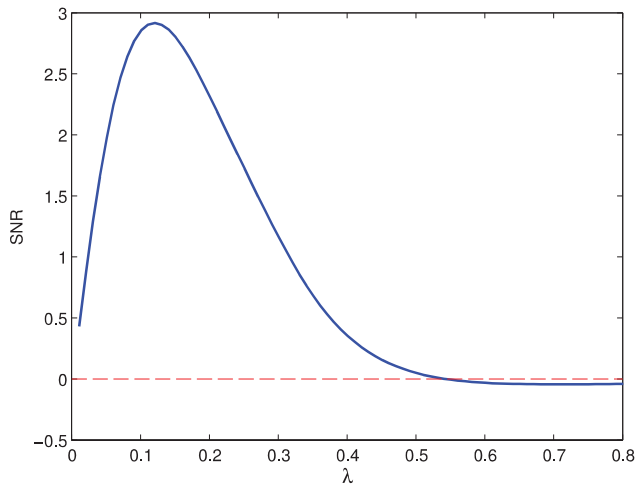


Figure 1. The influence of parameter  $\lambda$  on the signal to noise ratio.

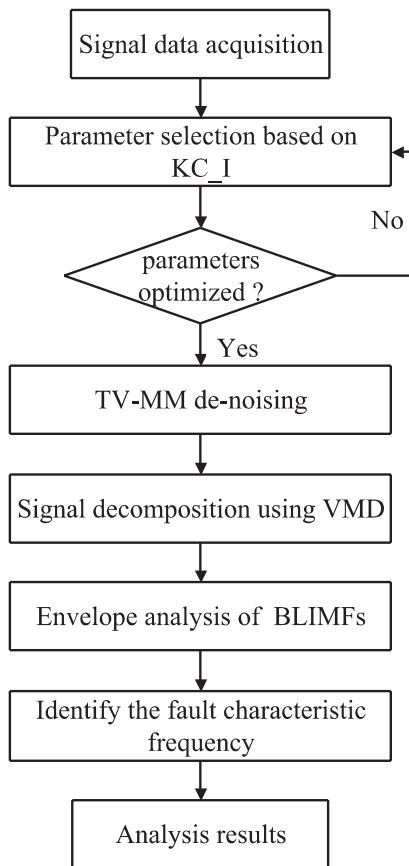


Figure 2. The flow chart of the proposed method.

performance will be very poor in this case. The influences of the parameter  $\lambda$  on the signal to noise ratio (SNR) are illustrated in figure 1. As can be seen in figure 1, a large value of  $\lambda$  will excessively remove noise as well as fine signatures, which results in a large kurtosis of the output signal. On the contrary, a small value of  $\lambda$  used in the algorithm will not effectively remove noise.

With regards to the selection of parameter  $\lambda$ , an approach has been described in [34] based on the Stein unbiased risk estimator (SURE). However, the noise variance  $\sigma^2$  is required for the SURE, while errors may be caused by the estimation of

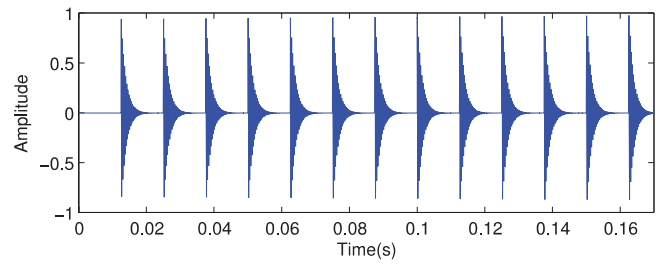


Figure 3. Simulated vibration signal  $s(t)$  without noise.

the noise variance. In addition,  $\lambda = \sqrt{3} \sigma$  is a usually used and verified experimentally in [31, 35]. In this work, a weighted kurtosis index approach is proposed to select a suitable  $\lambda$ . The weighted kurtosis index ( $KC_I$ ) is achieved by the kurtosis index ( $K_I$ ) and correlation coefficient index ( $C_I$ ), as represented in equation (11). As is well known, the kurtosis of the bearing vibration signal is a very important indicator, and its maximization is often adopted in fault diagnosis. Whereas it is not always appropriate to simply use kurtosis maximization as a signal denoising indicator. The reason is that features embedded in a given signal may be sometimes removed to some extent, if we only consider the kurtosis maximization criterion. Correlation coefficients, as a supplement, can ensure a certain similarity between the original signal and the denoised signal. Therefore, the proposed method can still ensure fidelity of the denoised signal. The regularization parameter  $\lambda$  is set to  $\lambda \geq 0$  which controls the smoothness of the signal. It can be seen in figure 1 that SNR is close to a constant value when  $\lambda \geq 0.6$  is satisfied. As a result,  $[0, 1]$  is selected as a region in order to get a more reasonable parameter  $\lambda$ . The process of the parameter  $\lambda$  selection is described as follows: First, the range of parameter  $\lambda$  is set to  $[0, 1]$ . Then, the maximum  $KC_I$  of the denoised signal will be searched in this region. Thus, the parameter  $\lambda$  value and the corresponding maximum  $KC_I$  are achieved. Finally, the value of parameter  $\lambda$  can be considered as an optimal parameter.

$$K_I = \frac{\frac{1}{n} \sum_{i=1}^N (x_i - \bar{x})^4}{\left( \frac{1}{n} \sum_{i=1}^N (x_i - \bar{x})^2 \right)^2} \quad (9)$$

$$C_I = \frac{\text{cov}(x, y)}{\sigma_x \sigma_y} = \frac{E((x - \bar{x})(y - \bar{y}))}{\sigma_x \sigma_y} \quad (10)$$

$$KC_I = K_I \times |C_I|^r \quad (11)$$

where  $r$  is an adjustable positive real number and is applied to add fidelity of the denoised signal. In this paper,  $r$  is set to 2 based on the results of the experiment.

### 3.2. TV-MM denoising combined with VMD

When the parameter  $\lambda$  used in the TV-MM algorithm is determined, a hybrid approach is developed to detect bearing fault based on the TV-MM and VMD. The proposed method for bearing fault diagnosis is schematically shown in figure 2.

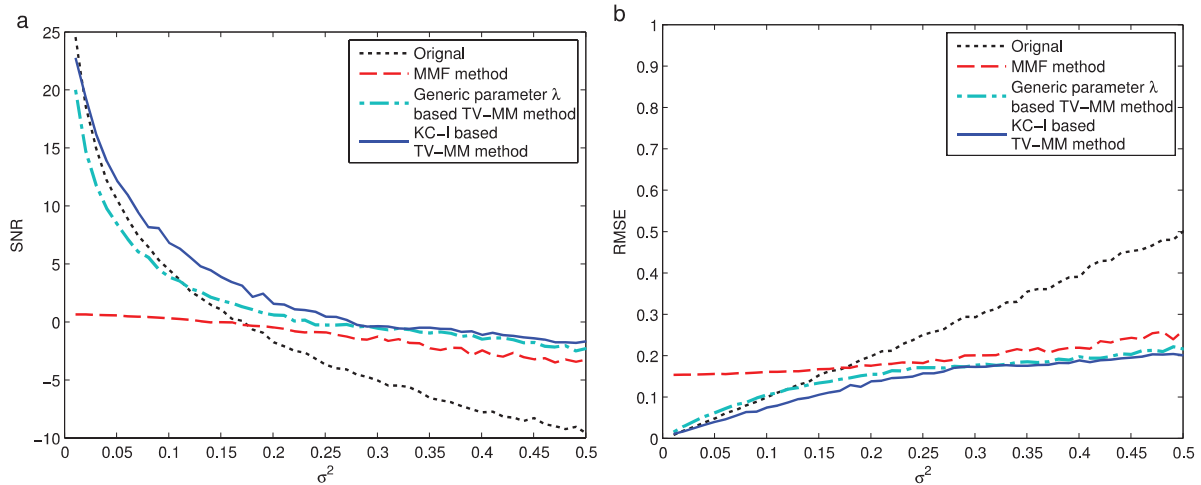


Figure 4. SNR and RMSE of the de-noised signal with TV-MM and MMF.

### 3.3. Validations and comparisons

Compared with total variation de-noising, the morphological morphology filter (MMF) has been initially used in image processing and has attracted lots of attention due to its little computation burden [36, 37]. To further evaluate the performance of the TV-MM method, it is compared with MMF through simulated signals in this section. A simulated signal of rolling bearing failure is written as follows:

$$s(t) = \sum_{k=0}^{\infty} A_k h(t - kT - \tau_k) + n(t) = x(t) + n(t) \quad (12)$$

$$A_k = 1 + A_0 \sin(2\pi f_r t) \quad (13)$$

$$h(t) = e^{-Ct} \sin(2\pi f_n t) \quad (14)$$

where  $x(t)$  is the original periodical impulsive signal, and  $n(t)$  is Gaussian white noise. The fault characteristic frequency  $f_0 = 1/T$ , random fluctuation of  $T$  due to slippage  $\tau_k$ , initial amplitude of the impulse  $A_0$ , rotational frequency  $f_r$ , decay factor  $C$  and resonant frequency  $f_n$  have been set to 80 Hz, 0, 0.3, 20 Hz, 700 and 3 kHz, respectively. In this paper, sampling frequency  $f_s$  is set to 12 kHz, and the data length is 2048.

The simulated signal  $s(t)$  without Gaussian white noise is shown in figure 3. The performance of the two denoising methods are evaluated based on SNR and the root mean square error (RMSE), which are defined below:

$$\text{SNR} = 10 \log \left\{ \frac{\sum_{i=1}^N s^2(i)^2}{\sum_{i=1}^N (s(i) - \hat{s}(i))^2} \right\} \quad (15)$$

$$\text{RMSE} = \sqrt{\frac{1}{N} \sum_{i=1}^N (s(i) - \hat{s}(i))^2} \quad (16)$$

in which  $s(i)$  ( $i = 1, 2, \dots, N$ ) is the original periodical signal, while  $\hat{s}(i)$  ( $i = 1, 2, \dots, N$ ) is the purified signal.

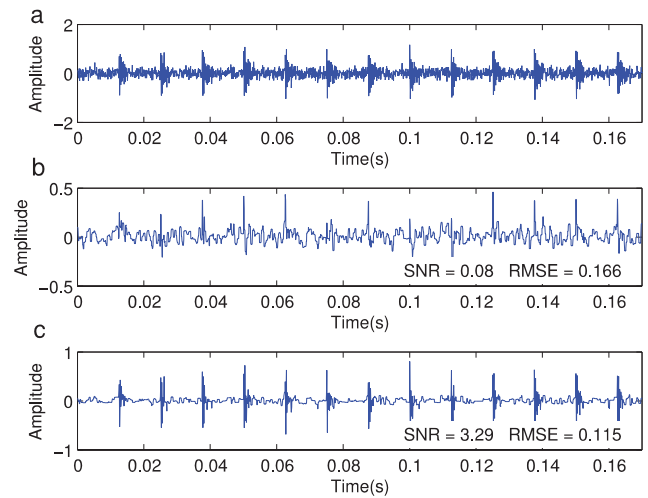


Figure 5. The time domain waveform of de-noising results obtained using two de-noising algorithms. (a) Original vibration signal, (b) the filtered signal with MMF, (c) the filtered signal with TV-MM.

It can be seen in figure 4 that the SNR and RMSE are better when parameter  $\lambda$  is selected based on the proposed weighted kurtosis index, rather than using the universal value ( $\lambda = \sqrt{3} \sigma$ ). Figure 4 also indicates that the TV-MM algorithm is much more effective than the MMF algorithm. In what follows, the SNR of a noisy signal with 1.5 dB is used to show its denoised waveforms. The results of the two methods are shown in figure 5. It can be seen that the TV-MM algorithm can eliminate noise and preserve impulsive characteristics as much as possible, but several features of the original signal are removed when MMF is adopted. Results indicate that the TV-MM algorithm outperforms MMF through the comparisons. Thus, TV-MM will be used as a preprocessing technique prior to VMD.

VMD is applied to decompose the denoised signal with TV-MM and MMF techniques, respectively. The decomposed four BLIMFs are shown in figure 6. VMD has a good ability to detect impacts hidden in a signal [22]. As is illustrated in figure 6, impulsive components have been well extracted. Meanwhile, the results indicate that figure 6(b) is better than

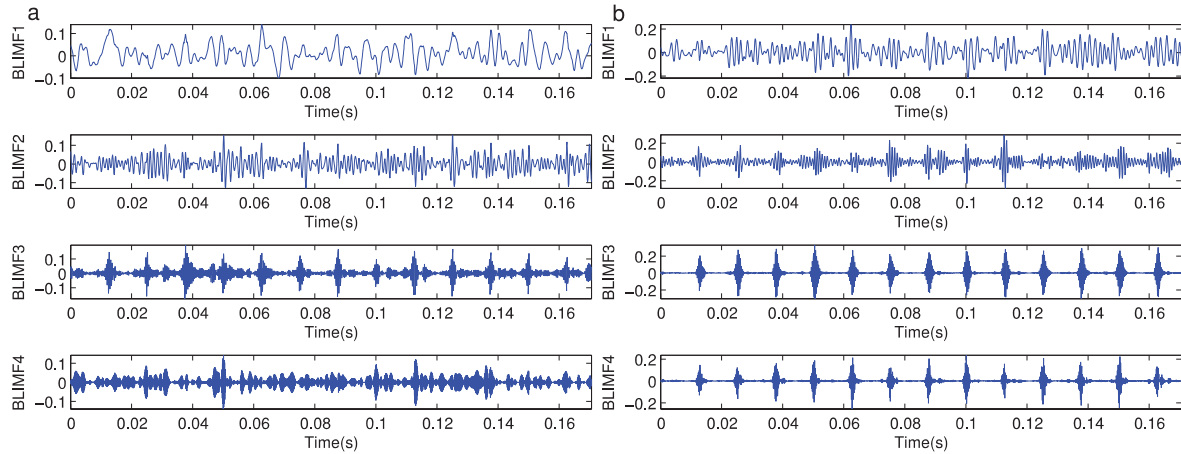


Figure 6. BLIMFs of the de-noised signal using VMD (a) denoising with MMF (b) denoising with TV-MM.

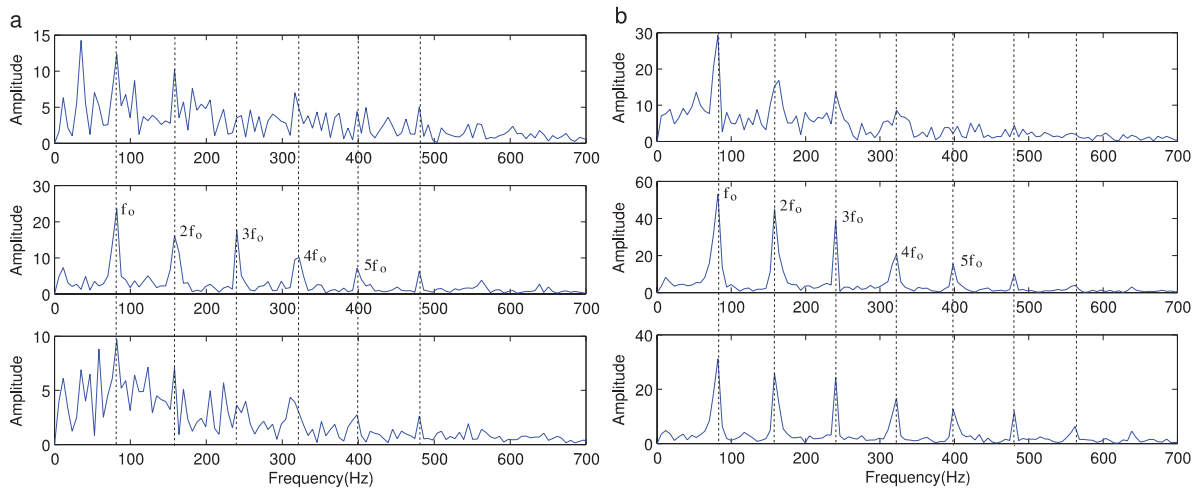


Figure 7. Envelopes of the BLIMF2, BLIMF3 and BLIMF4.

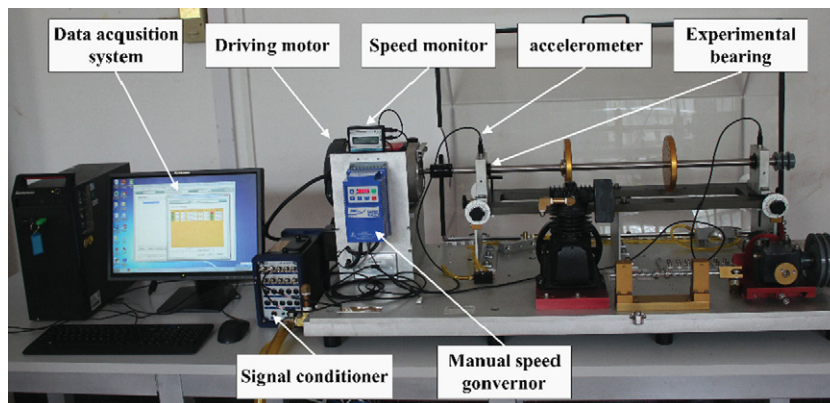


Figure 8. Machinery fault simulator (MFS)-magnum experimental platform.

figure 6(a), which demonstrates that the proposed hybrid technique is effective in detecting periodical impulsive signatures. Except for the first low-frequency BLIMF1 components, the Hilbert envelope spectra of the BLIMF2–BLIMF4 components are all shown in figure 7. Although both methods can extract the fault characteristic frequency, it is obvious that TV-MM combined with VMD can achieve a better performance than MMF. Its effectiveness will be further investigated using practical bearing vibration signals.

#### 4. Experimental evaluations

In this section, two kinds of bearing (outer race defect and inner race defect) signals acquired on an MFS-Magnum test-rig are adopted to verify the effectiveness of the proposed method. The test-rig is illustrated in figure 8. Type ER-12K bearings are used in the experiments, whose specifications are provided in table 1. Parameters relating to the fault signature are listed in table 2, in which the theoretical values

**Table 1.** Specifications of the bearing.

Inside diameter (mm)	Outside diameter (mm)	Pitch diameter (mm)	Number of rolling elements (mm)	Ball diameter (mm)
25.4	52	33.4772	8	7.9375

**Table 2.** Parameters related to fault.

Defect location	Rotational speed (r min <sup>-1</sup> )	Sampling frequency $f_s$ (kHz)	Rotation frequency $f_r$ (Hz)	Fault characteristic frequency (Hz)
Outer race	1790	12.8	29.83	90.96
Inner race	1792	25.6	29.87	147.84

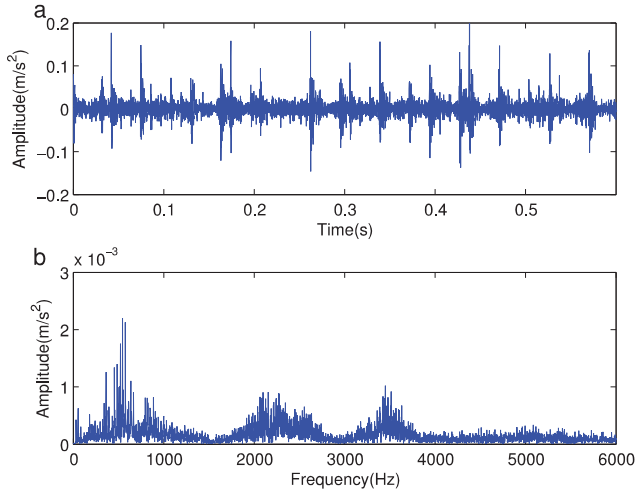


**Figure 9.** Vibration signal of bearing with an outer race fault (a) time domain waveform, (b) fast Fourier transform (FFT) spectrum.

of fault characteristic frequency are calculated via equations (17) and (18).

$$BPFO = \frac{N_b}{2} * f_r * \left( 1 - \frac{B_d}{P_d} * \cos \theta \right) \quad (17)$$

$$BPFI = \frac{N_b}{2} * f_r * \left( 1 + \frac{B_d}{P_d} * \cos \theta \right) \quad (18)$$

where BPFO denotes the ball passing frequency of the outer race, BPFI is the ball passing frequency of the inner race,  $N_b$  is the number of balls,  $f_r$  is the rotational frequency,  $B_d$  is the ball diameter,  $P_d$  is the pitch diameter, and  $\theta$  is the contact angle. Vibration data were collected using a VibraQuest data acquisition system with an accelerometer (sensitivity 98 mV g<sup>-1</sup>) fixed near the bearing bases.

#### 4.1. Bearing outer race fault detection

The raw vibration signal of the bearing with an outer race defect is shown in figure 9. As is well known, the vibration signal should present the impulsive features due to the presence of a defect in the rolling bearing. However, weak signatures in the time domain are often contaminated because of the existing strong ambient noises.

The purified signal using TV-MM is shown in figure 10. Compared with the original signal, noises are successfully

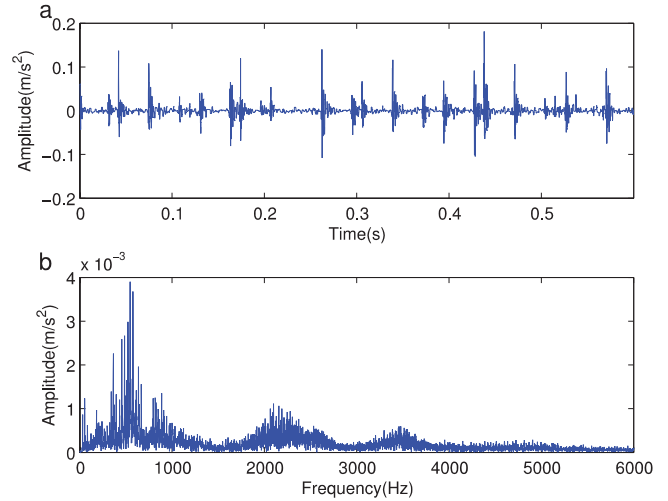


**Figure 10.** Result of TV-MM denoising (a) time-domain waveform, (b) its FFT spectrum.

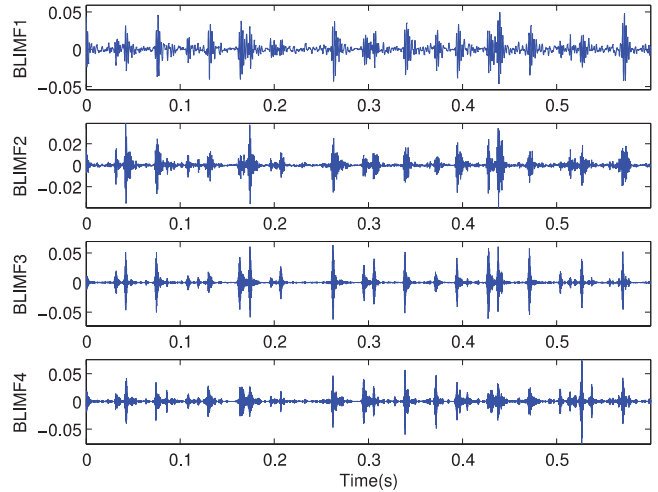


**Figure 11.** The decomposed BLIMFs of the purified signal using VMD.

removed in figure 10, and impulsive features are well retained. In addition, characteristic frequencies are concentrated in the low frequency band.

The VMD method is then applied to the purified signal, and the decomposed results are shown in figure 11. The envelope spectra of the BLIMF2–BLIMF4 are shown in figure 12. As is illustrated in figure 12, the rotating frequency  $f_r$  and the outer race fault characteristic frequency BPFO is clearly revealed.

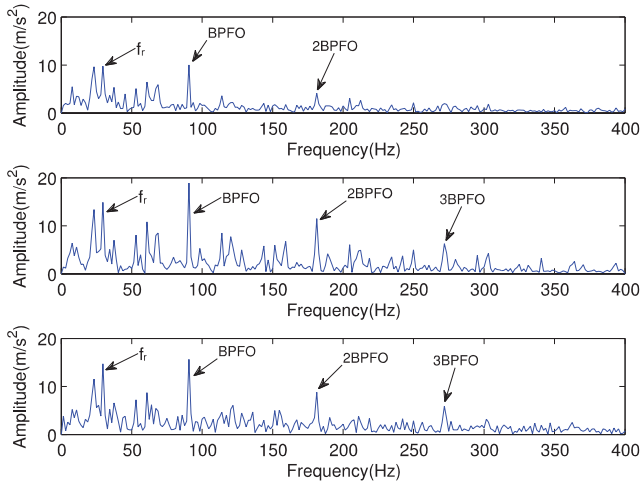


**Figure 12.** The envelope spectra of the BLIMF2–BLIMF4 (the purified signal with TV-MM).

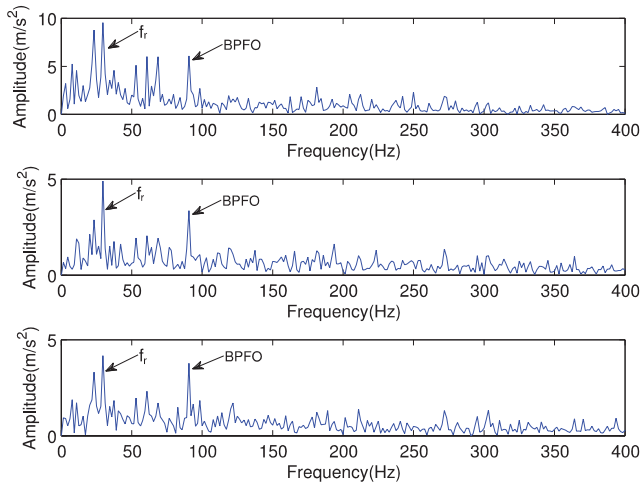


**Figure 13.** The envelope spectra of the latter three BLIMFs (the purified signal with MMF).

Moreover, the purified signal using MMF is also decomposed with VMD. The achieved Hilbert envelope spectra of the BLIMF2–BLIMF4 are shown in figure 13. It can be seen that the detected characteristic frequencies are not as good as those given in figure 12.

**4.2. Detection of bearing inner race fault**

In the case of the bearing inner race defect, the vibration signal is an amplitude modulated waveform due to the rotating of the inner race. Therefore, the side-band is expected at two frequencies, i.e.  $BPFI \pm f_r$ . The original vibration signal and the purified signal using TV-MM are presented in figures 14(a) and (b), respectively. The envelope spectrum of BLIMF4 is shown in figure 15(a), which contains the most abundant fault information among the four BLIMFs. In figure 15(a), it can be seen that BPFI, 2BPFI and 3BPFI along with the side bands ( $147.84 \pm 29.87$  Hz,  $295.68 \pm 29.87$  Hz,  $443.52 \pm 29.87$  Hz,  $591.36$  Hz +  $29.87$  Hz) are all prominent. It reveals that there exists an inner race fault

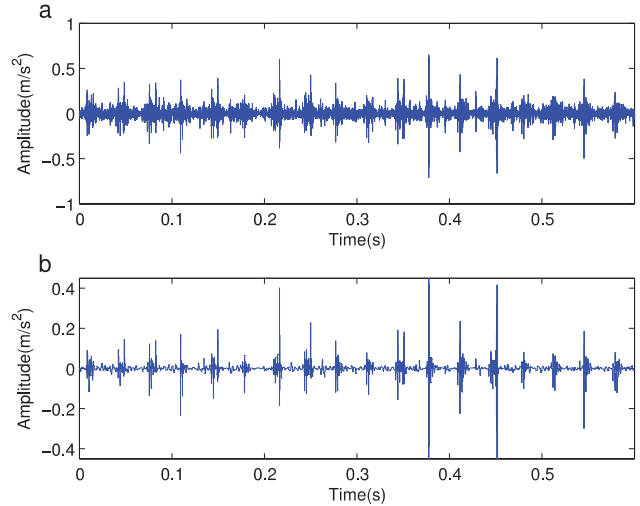


**Figure 14.** Vibration signal of bearing with an inner race fault (a) the raw signal, (b) the purified signal with TV-MM.

in the bearing. On the contrary, as is shown in figure 15(b), the envelope spectrum of BLIMF4 achieved by VMD and MMF can only indicate part of the signatures. In addition, it is also demonstrated that parameter  $\lambda$  selection technique based on the proposed weighted kurtosis index is appropriate for TV-MM denoising.

**5. Conclusions**

In this paper, the weighted kurtosis index is introduced into TV-MM de-noising, which can adaptively select an appropriate regularization parameter during the iterations. The de-noising results are better when the adaptive selection of  $\lambda$  is used in TV-MM, compared with the other general choice of  $\lambda$ . Moreover, a hybrid method which combines TV-MM and VMD is proposed to the bearing fault detection. VMD is applied to extract impulsive signatures of the purified signals via TV-MM denoising. The proposed hybrid approach is evaluated by simulated signals and real bearing vibration signals. A series of experimental tests corresponding to different bearing health conditions have demonstrated the superior capability of the proposed technique to the related classical bearing fault detection methods, especially in the aspect of denoising and non-stationary feature extraction.

**Acknowledgments**

The financial sponsorship from the project of the National Natural Science Foundation of China (51475098 and 61463010) and Guangxi Natural Science Foundation (2013GXNSFBA019238) are gratefully acknowledged. It is also sponsored by the Guangxi Experiment Center of Information Science (20130312) and Guangxi Key Laboratory of Manufacturing System & Advanced Manufacturing Technology (15-140-30-001Z).

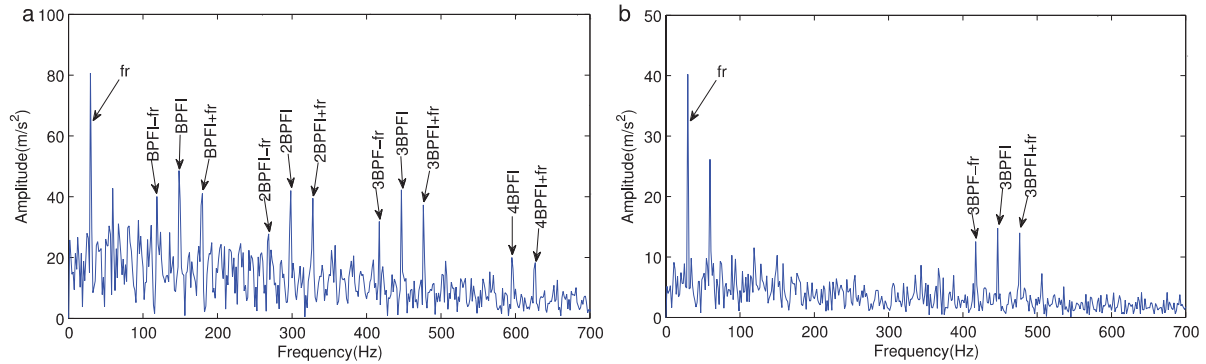


**Figure 15.** (a) The envelope spectrum of the fourth BLIMF (the purified signal with TV-MM), (b) the envelope spectrum of the fourth BLIMF (the purified signal with MMF).

## References

- [1] Osman S and Wang W 2013 An enhanced Hilbert–Huang transform technique for bearing condition monitoring *Meas. Sci. Technol.* **24** 085004
- [2] Wang W and Lee H 2013 An energy kurtosis demodulation technique for signal denoising and bearing fault detection *Meas. Sci. Technol.* **24** 025601
- [3] Chen B J, He Z J, Chen X F and Cao H R 2011 A demodulating approach based on local mean decomposition and its applications in mechanical fault diagnosis *Meas. Sci. Technol.* **22** 055704
- [4] Fan X F and Zuo M J 2008 Machine fault feature extraction based on intrinsic mode functions *Meas. Sci. Technol.* **19** 045105
- [5] Liu Y, Zhang J H, Bi F G, Lin J W and Ma W P 2015 A fault diagnosis approach for diesel engine valve train based on improved ITD and SDAG-RVM *Meas. Sci. Technol.* **26** 025003
- [6] Lei Y G, Dong H, Jing L and He Z 2013 Planetary gearbox fault diagnosis using an adaptive stochastic resonance method *Mech. Syst. Signal Process.* **38** 113–24
- [7] Randall R B and Antoni J 2011 Rolling element bearing diagnostics—a tutorial *Mech. Syst. Signal Process.* **25** 485–520
- [8] Liu J, Wang W, Golnaraghi F and Liu K 2007 Wavelet spectrum analysis for bearing fault diagnostics *Meas. Sci. Technol.* **19** 015105
- [9] Abbasion S, Rafsanjani A, Farshidianfar A and Irani N 2007 Rolling element bearings multi-fault classification based on the wavelet denoising and support vector machine *Mech. Syst. Signal Process.* **21** 2933–45
- [10] Yan R Q, Gao R X and Chen X F 2014 Wavelets for fault diagnosis of rotary machines: a review with applications *Signal Process.* **96** 1–15
- [11] Huang N E, Shen Z, Long S R, Wu M C, Shih H H, Yen N C, Tung C C and Liu H H 1998 The empirical mode decomposition and the Hilbert spectrum for nonlinear and non-stationary time series analysis *Proc. R. Soc. A* **454** 903–95
- [12] He Q B, Liu Y B and Kong F R 2010 Machine fault signature analysis by midpoint-based empirical mode decomposition *Meas. Sci. Technol.* **22** 015702
- [13] Wu T Y, Chen J C and Wang C C 2012 Characterization of gear faults in variable rotating speed using Hilbert–Huang transform and instantaneous dimensionless frequency normalization *Mech. Syst. Signal Process.* **30** 103–22
- [14] Yang W and Tavner P J 2009 Empirical mode decomposition, an adaptive approach for interpreting shaft vibratory signals of large rotating machinery *J. Sound Vib.* **321** 1144–70
- [15] Rilling G, Flandrin P and Goncalves P 2003 On empirical mode decomposition and its algorithms *IEEE-EURASIP Workshop Nonlinear Signal Image Processing (NSIP)* vol 3 pp 8–11
- [16] Rilling G and Flandrin P 2009 Sampling effects on the empirical mode decomposition *Adv. Adapt. Data Anal.* **1** 43–59
- [17] Chen G and Wang Z 2012 A signal decomposition theorem with Hilbert transform and its application to narrowband time series with closely spaced frequency components *Mech. Syst. Signal Process.* **28** 258–79
- [18] Guo W and Tse P W 2010 Enhancing the ability of ensemble empirical mode decomposition in machine fault diagnosis *Proc. IEEE Conf. Prognostics Health Management PHM'10* pp 1–7
- [19] Lei Y G and Zuo M J 2009 Fault diagnosis of rotating machinery using an improved HHT based on EEMD and sensitive IMFs *Mech. Sci. Technol.* **20** 125701
- [20] Gilles J 2013 Empirical wavelet transform *IEEE Trans. Signal Process.* **61** 3999–4010
- [21] Dragomiretskiy K and Zosso D 2014 Variational mode decomposition *IEEE Trans. Signal Process.* **62** 531–44
- [22] Wang Y X and Markert R 2016 Filter bank property of variational mode decomposition and its applications *Signal Process.* **120** 509–21
- [23] Upadhyay A and Pachori R B 2015 Instantaneous voiced/non-voiced detection in speech signals based on variational mode decomposition *J. Franklin Inst.* **352** 2679–707
- [24] Aneesh C, Kumar S, Hisham P M and Soman K P 2015 Performance comparison of variational mode decomposition over empirical wavelet transform for the classification of power quality disturbances using support vector machine *Proc. Comput. Sci.* **46** 372–80
- [25] Wang Y X, Markert R, Xiang J W and Zheng W G 2015 Research on variational mode decomposition and its application in detecting rub-impact fault of the rotor system *Mech. Syst. Signal Process.* **60** 243–51
- [26] Lahmiri S 2015 Long memory in international financial markets trends and short movements during 2008 financial crisis based on variational mode decomposition and detrended fluctuation analysis *Physica A* **437** 130–8
- [27] Rudin L I, Osher S and Fatemi E 1992 Nonlinear total variation based noise removal algorithms *Physica D* **60** 259–68
- [28] Karahanoğlu F I, Bayram I and Van De Ville D 2011 A signal processing approach to generalized 1D total variation *IEEE Trans. Signal Process.* **59** 5265–74
- [29] Condat L 2013 A direct algorithm for 1D total variation denoising *IEEE Trans. Signal Process. Lett.* **20** 1054–7
- [30] Ning X and Selesnick I W 2013 ECG enhancement and QRS detection based on sparse derivatives biomed *Signal Process. Control.* **8** 713–23

- [31] Figueiredo M A T, Dias J B, Oliveira J P and Nowak R D 2006 On total variation denoising: a new majorization-minimization algorithm and an experimental comparison with wavelet denoising *Proc. IEEE Int. Conf. Image Process.* pp 2633–6
- [32] Selesnick I 2012 *Total variation denoising (an MM algorithm)* NYU Polytechnic School of Engineering Lecture Notes. ([http://eeweb.poly.edu/iselesni/lecture\\_notes/](http://eeweb.poly.edu/iselesni/lecture_notes/))
- [33] Daubechies I, Lu J and Wu H T 2011 Synchrosqueezed wavelet transforms: an empirical mode decomposition-like tool *Appl. Comput. Harmon. Anal.* **30** 243–61
- [34] Karahanoğlu F I, Bayram I and Van De Ville D 2013 Local behavior of sparse analysis regularization: applications to risk estimation *Appl. Comput. Harmon. Anal.* **35** 433–51
- [35] Figueiredo M A T and Nowak R D 2001 Wavelet-based image estimation: an empirical Bayes approach using Jeffreys' noninformative prior *IEEE Trans. Image Proc.* **10** 1322–31
- [36] Wang J, Xu G H, Zhang Q and Liang L 2009 Application of improved morphological filter to the extraction of impulsive attenuation signals *Mech. Syst. Signal. Process.* **23** 236–45
- [37] Meng L J, Xiang J W, Wang Y X, Jiang Y Y and Gao H F 2015 A hybrid fault diagnosis method using morphological filter-translation invariant wavelet and improved ensemble empirical mode decomposition *Mech. Syst. Signal. Process.* **50–1** 101–15